DOI: 10.1002/cmdc.200700281

A Small Molecular Scaffold for Selective Inhibition of Wip1 Phosphatase**

Jeong Bang,[b] Hiroshi Yamaguchi,[b] Stewart R. Durell,[b] Ettore Appella,[b] and Daniel H. Appella*[a]

The phosphatase Wip1 (also called PP2Cδ) indirectly suppresses the activity of the tumor suppressor protein p53.[1] After DNA damage, such as ionizing radiation or UV light, several cellular pathways combine to increase the activity of p53, which in turn controls cell cycle arrest and apoptosis. Within the network of p53 activation, Wip1 inactivates p38 MAP kinase by dephosphorylation of a phosphothreonine. In its own role, phosphorylated p38 MAP kinase phosphorylates and activates p53. Therefore, Wip1 controls a negative feedback loop within the p38 MAP kinase–p53 signaling pathway. Other roles for Wip1 include suppression of Chk2 activity, a kinase controlling the G2/M DNA damage checkpoint.[2] Overexpression of Wip1 protein (and amplification of its associated gene PPM1D) has been observed in several cancers, including breast cancer, neuroblastoma, and ovarian clear cell adenocarcinoma. Furthermore, the PPM1D gene complements other well-known oncogenes such as Ras, ErbB2, and Myc for cellular transformations of primary mouse embryo fibroblasts.[3] The data accumulated about the biological functions of Wip1 indicate that inhibition of its enzymatic activity could be an effective strategy for combating certain types of cancer.

Although the three-dimensional structure of Wip1 has not yet been determined, it is a member of the protein phosphatase 2C (PP2C) family and bears significant homology to the protein PP2Cα whose crystal structure has been determined.[4] However, homology-based models of Wip1 necessarily exclude residues 239–263 of the protein because this segment is unique among the sequence alignments of PP2C family members and thus there is no template to model this section from the PP2Cα crystal structure. These unique residues likely form a loop on the protein surface near the periphery of the catalytic site, and possibly convey substrate specificity to Wip1. In this regard, two classes of substrate have been identified for Wip1: diphosphorylated peptides typified by p38 MAP kinase, and monophosphorylated peptides typified by ATM.[5] The former substrate class has pTXpY polypeptide sequences (where pT and pY represent phosphorylated threonine and tyrosine respectively, and X denotes a hydrophobic amino acid). In this case, the pT residue is selectively dephosphorylated while the pY residue forms a stabilizing salt bridge with K238 of the protein, which is a residue unique to Wip1. The latter class of substrates for Wip1 has a pSQ motif (pS denotes phosphoserine). In this case, stabilizing interactions between Q and D264 of Wip1 (also unique to Wip1) promote selectivity. It is important to note that the optimal substrates of Wip1 are different from those of PP2Cα. To date, only a handful of successful Wip1 inhibitors have been described.[6] These types of inhibitors include peptide and cyclic peptide-based molecules, an organomercuric compound, and an electrophilic molecule that is a strong Michael acceptor. As a result of the metabolic instability of peptides and the toxicity associated with mercury and highly electrophilic molecules, the current Wip1 inhibitors are not likely to be developed as drug candidates.

In this study, we report the design, synthesis, and characterization of a small, druglike, molecular scaffold for the selective inhibition of Wip1. The inhibitors are based on the cyclic peptide c(MpSIpYVA) (Figure 1 A), which inhibits Wip1 with a K_i of $< 1\ \mu M$, but is not highly selective for Wip1 over PP2Cα. More selective cyclic peptide inhibitors have been developed, but at the expense of Wip1 inhibition.[6b]

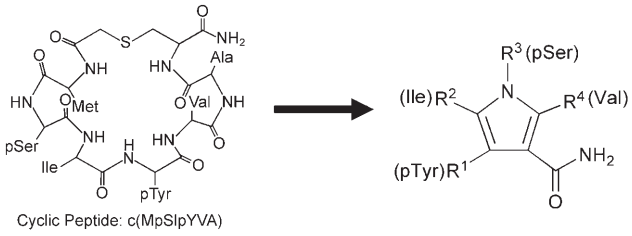

Figure 1. A) Chemical structure of c(MpSIpYVA), B) pyrrole scaffold to mimic the cyclic peptide (side chain mimics labeled in parentheses).

To develop a small organic analogue of c(MpSIpYVA), groups mimicking the phosphotyrosine, phosphoserine, isoleucine, and valine residues of the cyclic peptide need to be present on the new scaffold. The pyrrole-based molecules of the type shown in Figure 1 B represent the scaffold we chose for development of a small molecule inhibitor of Wip1. Among the pyrrole side chains, R^1 and R^3 were assigned as the positions from which phosphate groups would be attached, and side chains R^2 and R^4 were assigned as the positions to attach hydrophobic groups.

To make the pyrrole derivatives, a synthetic route was developed based on known procedures to make pyrroles (Scheme 1).[7] Initially, β-ketoamides were synthesized on a solid support by the combination of Rink amide resin with acylated derivatives of Meldrum's acid. Next, addition of an amine to form an enaminone on the solid support, followed by addition of an α,β-unsaturated nitroalkene resulted in pyrrole for-

[a] Dr. D. H. Appella
Laboratory of Bioorganic Chemistry
NIDDK, NIH, DHHS
Bethesda, MD 20892 (USA)
Fax: (+1) 301-480-4977
E-mail: appellad@niddk.nih.gov

[b] Dr. J. Bang, Dr. H. Yamaguchi, Dr. S. R. Durell, Dr. E. Appella
Laboratory of Cell Biology, NCI
Bethesda, MD 20892 (USA)

[**] This work was supported in part by the Intramural Research Programs at NIDDK and NCI, NIH.

Supporting information for this article is available on the WWW under http://www.chemmedchem.org or from the author.

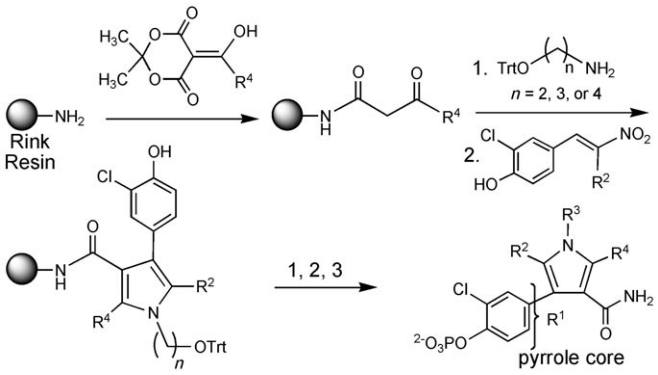

Scheme 1. Synthetic route for pyrrole derivatives. 1) trityl deprotection; 2) Phosphorylation; 3) Cleavage from resin

mation. Deprotection, followed by phosphorylation and cleavage from the resin afforded the target pyrroles. Using this route, 27 different pyrroles were made and tested as inhibitors for Wip1 (see Supporting Information for complete details), and the positions around the pyrrole ring were optimized for inhibition.

In Table 1, the Wip1 inhibition constants (K_i) are shown for 11 of the pyrrole derivatives. For R^1, the optimal group is a 2-chloro-phenylphosphate (see Scheme 1), and all the entries in Table 1 have this group at R^1. Optimization then proceeded with R^2. Several hydrophobic groups were examined, but alkyl chains with a branched methyl group were superior to straight chain alkyl groups (compare entries 1 to 2 and 3, Table 1). A 2-methylpentyl group was chosen as a side chain for this position. Optimization at R^3 (the mimic for phosphoserine) focused on finding the ideal distance between the phosphate group and the pyrrole core. As shown in Table 1, this distance was clearly 3 methylene units (compare entries 3, 4, and 5, Table 1). Next, optimization at R^4 determined that chloro-aromatic groups at this position were ideal (entries 6, 7, and 8, Table 1). Finally, each enantiomer of the 2-methylpentyl side chain was prepared, and the (*S*) enantiomer was clearly more active than (*R*). The chirality of the molecule was eliminated by replacing the 2-methylpentyl side chain with 2-propylpentyl and Wip1 inhibition improved slightly.

Finally, the selectivity of the best inhibitors of Wip1 (Table 1, entries 8, 9, 10) was tested against PP2Cα and a K238D mutant of Wip1. These molecules showed no detectable inhibition of either protein, demonstrating that these compounds are highly selective.

The current model we propose for the binding of the pyrrole from entry 9 to Wip1 is presented in Figures 2 and 3. Comparison with the bound conformation of c(MpSIpYVA) (Figure 2) indicates that the chlorophenylphosphate group in position R^1 likely mimics the phosphotyrosine, and also contacts K238 of the Wip1 protein. This is a unique residue within Wip1, and is required for substrate selectivity. The inability of our molecule to inhibit the K238D mutant of Wip1 reinforces this idea. The other phosphate group (position R^3) likely mimics the phosphoserine and contacts R76 and the metal–ligand complex (Figure 3). The 2-methylpentyl side chain mimics the isoleucine in the cyclic peptide, but there is no clear site of interaction of this side chain with the protein. In the model, this side chain projects above the plane of the picture and could interact with the unique series of Wip1 residues that we propose forms a loop over the catalytic site. The chloroaromatic side chain interacts with F268, and the primary amide interacts with D264, residues that are both unique to Wip1.

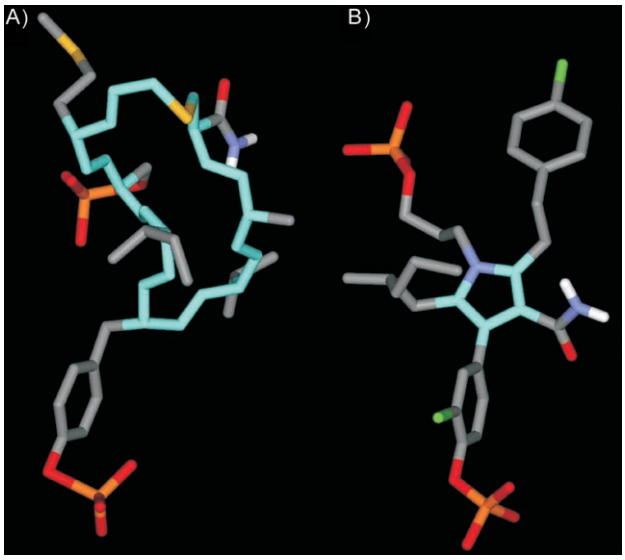

Figure 2. Comparison of A) bound cyclic peptide with B) entry 9.

Table 1. Pyrrole analogues synthesized and tested for Wip1 inhibition.

Entry[a]	R^2	R^3	R^4	K_i [μM][b]
1	*n*-C_5H_{11}	-$(CH_2)_2OPO_3^{2-}$	CH_3	77 ± 12
2	$CH_2CH(CH_3)_2$	-$(CH_2)_2OPO_3^{2-}$	CH_3	38 ± 8
3	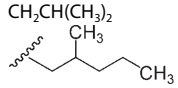	-$(CH_2)_2OPO_3^{2-}$	CH_3	40 ± 1
4	2-methylpentyl	-$(CH_2)_3OPO_3^{2-}$	CH_3	17 ± 1
5	2-methylpentyl	-$(CH_2)_4OPO_3^{2-}$	CH_3	NI[c]
6	2-methylpentyl	-$(CH_2)_3OPO_3^{2-}$	$CH_2CH(CH_3)_2$	43 ± 3
7	2-methylpentyl	-$(CH_2)_3OPO_3^{2-}$	CH_2(p-Cl-Phenyl)	6.2 ± 0.6
8	2-methylpentyl	-$(CH_2)_3OPO_3^{2-}$	$(CH_2)_2$(p-Cl-Phenyl)	5.7 ± 0.4
9	(*S*)-2-methylpentyl	-$(CH_2)_3OPO_3^{2-}$	$(CH_2)_2$(p-Cl-Phenyl)	4.7 ± 0.7
10	(*R*)-2-methylpentyl	-$(CH_2)_3OPO_3^{2-}$	$(CH_2)_2$(p-Cl-Phenyl)	10 ± 1
11	2-propylpentyl	-$(CH_2)_3OPO_3^{2-}$	CH_2(p-Cl-Phenyl)	4.0 ± 0.2

[a] See Scheme 1 for chemical structure of pyrrole core. [b] Phosphatase activity was measured as described in the experimental section. [c] No inhibition observed.

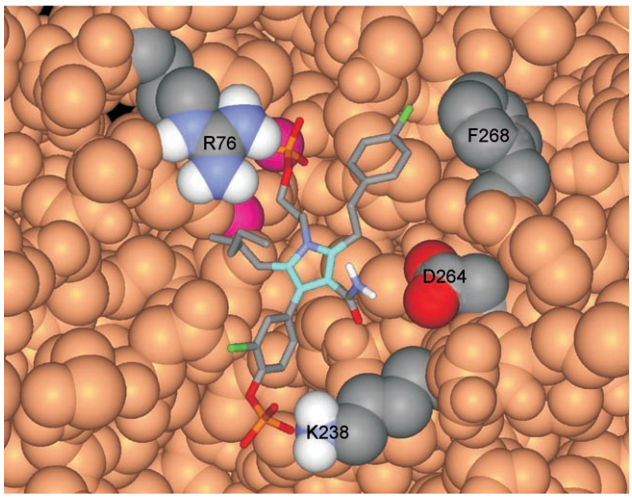

Figure 3. Model of Pyrrole 9 bound to Wip1. Residues K238, D264, and F268 are unique to Wip1.

In conclusion, we were able to generate selective inhibitors of Wip1, indicating that Wip1 is a good target for future drug development. The unique residues of Wip1 allowed us to synthesize small molecules that selectively bind to this phosphatase over others. It is our hope that these results will become the basis for development of future therapeutics to treat cancer.

Experimental Section

Synthesis and characterization of all pyrrole inhibitors is described in the Supporting Information. In the molecular modeling of the Wip1–Inhibitor complex, the atomic-scale, computer model of the active site of Wip1 was the same as described previously.[5,6b] This was a homology model developed from the crystal structure of PP2Cα.[4] Topology files and initial coordinates of the different pyrrole-based inhibitors were made with the 2-D Sketcher and 3-D Builder modules of the Quanta-2006 molecular modeling program (Accelrys Inc.: http://www.accelrys.com/). Energy minimization calculations were then done with the CHARMM (c31b2) molecular mechanics software package[8] using the "par_all22_prot" parameter set.[9] Phosphatase activity was measured by a malachite green/molybdate-based assay.[5] The IC_{50} values for inhibition of phosphatase activity by the phosphopeptide inhibitors were measured using 30 μM AFEEGpSQSTTI substrate peptide (residues 1976–1986 in human ATM kinase) for 7 min at 30 °C in 50 mM Tris-HCl, pH 7.5, 0.1 mM EGTA, 0.02% 2-mercaptoethanol, 40 mM NaCl, 30 mM $MgCl_2$. The phosphatase and phosphopeptide inhibitors were pre-equilibrated at 30 °C for 6 min. The inhibition percentages were estimated by Equation (1).

$$\text{Inhibition } (\%) = 100[1-(A-A_0)/(A_{100}-A_0)] \quad (1)$$

In Equation (1), A and A_{100} are absorbance intensities at 650 nm with or without the peptide inhibitor, respectively. A_0 is absorbance of the sample without phosphatase. The IC_{50} values were estimated by a sigmoidal dose-response equation. The apparent inhibitory constant K_i values were estimated using equation.[10]

$$K_i = IC_{50}/(1 + [S]/K_m) \quad (2)$$

In Equation (2), [S] is the concentration of the substrate peptide and K_m is the Michaelis constant.

Keywords: enzyme inhibition · organic synthesis · pyrrole · small molecules · Wip1

[1] a) M. Fiscella, H. Zhang, S. Fan, K. Sakaguchi, S. Shen, W. E. Mercer, G. F. V. Woude, P. M. O'Connor, E. Appella, *Proc. Natl. Acad. Sci. USA* **1997**, *94*, 6048–6053; b) D. V. Bulavin, S. I. Saito, M. C. Hollander, K. Sakaguchi, C. W. Anderson, E. Appella, A. J. Fornace, Jr., *EMBO J.* **1999**, *18*, 6845–6854; c) M. Takekawa, M. Adachi, A. Nakahata, I. Nakayama, F. Itoh, H. Tsukuda, Y. Taya, K. Imai, *EMBO J.* **2000**, *19*, 6517–6526.

[2] a) A. Yoda, X. Z. Xu, N. Onishi, K. Toyoshima, H. Fujimoto, N. Kato, I. Oishi, T. Kondo, Y. Minami, *J. Biol. Chem.* **2006**, *281*, 24847–24862; b) M. Oliva-Trastoy, V. Berthonaud, A. Chevalier, C. Ducrot, M.-C. Marsolier-Kergoat, C. Mann, F. Leteurtre, *Oncogene* **2007**, *26*, 1449–1458.

[3] a) J. Li, Y. Yang, Y. Peng, R. J. Austin, W. G. van Eyndhoven, K. C. Q. Nguyen, T. Gabriele, M. E. McCurrach, J. R. Marks, T. Hoey, S. W. Lowe, S. Powers, *Nat. Genet.* **2002**, *31*, 133–134; b) D. V. Bulavin, O. N. Demidov, S. I. Saito, P. Kauraniemi, C. Phillips, S. A. Amundson, C. Ambrosino, G. Sauter, A. R. Nebreda, C. W. Anderson, A. Kallioniemi, A. J. Fornace, Jr., E. Appella, *Nat. Genet.* **2002**, *31*, 210–215; c) A. Hirasawa, F. Saito-Ohara, J. Inoue, D. Aoki, N. Susumu, T. Yokoyama, S. Nozawa, J. Inazawa, I. Imoto, *Clin. Cancer Res.* **2003**, *9*, 1995–2004; d) S. Shreeram, W. K. Hee, O. N. Demidov, C. Kek, H. Yamaguchi, A. J. Fornace, Jr., C. W. Anderson, E. Appella, D. V. Bulavin, *J. Exp. Med.* **2006**, *203*, 2793–2799; e) O. N. Demidov, C. Kek, S. Shreeram, O. Timofeev, A. J. Fornace, Jr., E. Appella, D. V. Bulavin, *Oncogene* **2007**, *26*, 2502–2506.

[4] A. K. Das, N. R. Helps, P. T. W. Cohen, D. Barford, *EMBO J.* **1996**, *15*, 6798–6809.

[5] a) H. Yamaguchi, G. Minopoli, O. N. Demidov, D. K. Chatterjee, C. W. Anderson, S. R. Durell, E. Appella, *Biochemistry* **2005**, *44*, 5285–5294; b) H. Yamaguchi, S. R. Durell, D. K. Chatterjee, C. W. Anderson, E. Appella, *Biochemistry* **2007**, *46*, 12594–12603.

[6] a) G. I. Belova, O. N. Demidov, A. J. Fornace, Jr., D. V. Bulavin, *Cancer Biol. Ther.* **2005**, *4*, 1154–1158; b) H. Yamaguchi, S. R. Durell, H. Feng, Y. Bai, C. W. Anderson, E. Appella, *Biochemistry* **2006**, *45*, 13193–13202; c) S. Rayter, R. Elliott, J. Travers, M. G. Rowlands, T. B. Richardson, K. Boxall, K. Jones, S. Linardopoulos, P. Workman, W. Aherne, C. J. Lord, A. Ashworth, *Oncogene* **2007**, *26*, 1–9.

[7] a) H. Meyer, *Liebigs Ann. Chem.* **1981**, 1534–1544; b) H. Jendralla, E. Baader, W. Bartmann, G. Beck, A. Bergmann, E. Granzer, B. v. Kerekjarto, K. Kesseler, R. Krause, W. Schubert, G. Wess, *J. Med. Chem.* **1990**, *33*, 61–70; c) A. W. Trautwein, G. Jung, *Tetrahedron Lett.* **1998**, *39*, 8263–8266.

[8] B. R. Brooks, R. E. Bruccoleri, B. D. Olafson, D. J. States, S. Swaminathan, M. Karplus, *J. Comput. Chem.* **1983**, *4*, 187–217.

[9] A. D. MacKerell, Jr., D. Bashford, M. Bellott, R. L. Dunbrack, Jr., J. D. Evanseck, M. J. Field, S. Fischer, J. Gao, H. Guo, S. Ha, D. Joseph-McCarthy, L. Kuchnir, K. Kuczera, F. T. K. Lau, C. Mattos, S. Muchnick, T. Ngo, D. T. Nguyen, B. Prodhom, W. E. Reiher III, B. Roux, M. Schlenkrich, J. C. Smith, R. Stote, J. Straub, M. Watanabe, J. Wiorkiewicz-Kuczera, D. Yin, M. Karplus, *J. Phys. Chem. B* **1998**, *102*, 3586–3613.

[10] Y.-C. Cheng, W. H. Prusoff, *Biochem. Pharmacol.* **1973**, *22*, 3099–3108.

Received: October 5, 2007
Revised: October 22, 2007
Published online on November 19, 2007

